Gut Microbiome Dysbiosis is Associated with Increased Mortality following Solid Organ Transplantation

Rinse Weersma (r.k.weersma@umcg.nl)
University of Groningen and University Medical Center Groningen
J. Casper Swarte
University of Groningen and University Medical Center Groningen https://orcid.org/0000-0002-3709-9193
Yanni Li
University of Groningen and University Medical Center Groningen
Shixian Hu
University Medical Center Groningen
Johannes Björk
University of Groningen and University Medical Center Groningen
Ranko Gacesa
University of Groningen and University Medical Center Groningen
Arnau Vich Vila
University of Groningen and University Medical Center Groningen
Rianne Douwes
University of Groningen and University Medical Center Groningen
Valerie Collij
University of Groningen and University Medical Center Groningen
Alexander Kurilshikov
University Medical Center Groningen https://orcid.org/0000-0003-2541-5627
Adrian Post
University of Groningen and University Medical Center Groningen
Marjolein Klaassen
University of Groningen and University Medical Center Groningen
Michele Eisenga
University of Groningen and University Medical Center Groningen
António Gomes-Neto
University of Groningen and University Medical Center Groningen
Daan Kremer

University of Groningen and University Medical Center Groningen https://orcid.org/0000-0003-0011-115X

Bernadien Jansen
University of Groningen and University Medical Center Groningen

Tim Knobbe
University of Groningen and University Medical Center Groningen https://orcid.org/0000-0003-3246-3192

Stefan Berger
University of Groningen and University Medical Center Groningen

Jan-Stephan Sanders
University of Groningen and University Medical Center Groningen

M. Heiner-Fokkema
University of Groningen and University Medical Center Groningen

Robert Porte
University of Groningen and University Medical Center Groningen

Frans Cuperus
University of Groningen and University Medical Center Groningen

Vincent de Meijer
University of Groningen and University Medical Center Groningen https://orcid.org/0000-0002-7900-5917

Cisca Wijmenga
University Medical Centre Groningen https://orcid.org/0000-0002-5635-1614

Eleonora Festen
University of Groningen and University Medical Center Groningen

Alexandra Zhernakova
University of Groningen, University Medical Center Groningen, Department of Genetics, Groningen, the Netherlands

Jingyuan Fu
University Medical Center Groningen

Hermie Harmsen
The University of Groningen https://orcid.org/0000-0003-2725-6148

Hans Blokzijl
University of Groningen and University Medical Center Groningen

Stephan Bakker
University Medical Center Groningen https://orcid.org/0000-0003-3356-6791

Article

Keywords: Gut microbiome, organ transplantation, immunosuppressive medication, mortality, dysbiosis

Posted Date: February 5th, 2021

DOI: https://doi.org/10.21203/rs.3.rs-185980/v1

Abstract

Organ transplantation is a life-saving treatment for patients with end-stage disease, but survival post-transplantation varies considerably. There is now increasing evidence that the gut microbiome is linked to the survival of hematopoietic cell transplant patients, yet little is known about the role of the gut microbiome in solid organ transplantation. We analyzed 1,370 fecal samples from liver and renal transplant recipients using shotgun metagenomic sequencing to assess microbial taxonomy, metabolic pathways, antibiotic resistance genes and virulence factors. To quantify taxonomic and metabolic dysbiosis, we analyzed 1,183 age-, sex- and BMI-matched subjects from the same population. A subset of patients were also followed longitudinally from pre- to post-transplantation. Our data show that transplant recipients suffer from gut dysbiosis—including lower microbial diversity, increased abundance of unhealthy microbial species, decreased abundance of important metabolic pathways, and increased prevalence and diversity of antibiotic resistant genes and virulence factors—that persist up to 20 years post-transplantation. Finally, we demonstrate that the use of immunosuppressive drugs is significantly associated with the observed dysbiosis and that the extent of dysbiosis is associated with increased post-transplant mortality.

Introduction

Solid organ transplantation is a life-saving treatment for patients with acute or chronic liver and kidney failure (hereafter end-stage liver and renal disease)[1]. Despite improved surgical techniques and the introduction of potent immunosuppressive drugs, solid organ transplant recipients still suffer from rejections, infection and increased mortality [2,3]. The gut microbiome is involved in host immune homeostasis, and its resilience to perturbations protects against gut dysbiosis—a condition typically characterized by the growth of pathogens at the expense of commensal bacteria when compared to a healthy microbiota [4,5]. Such dysbiosis has previously been reported in both end-stage liver disease (ESLD) and end-stage renal disease (ESRD) [6,7]. However, the resistance of the gut microbiome to withstand both the direct and indirect changes associated with liver or renal transplantation and its link to recipient survival have not yet been comprehensively investigated. The microbiota of liver and renal transplant recipients (LTR and RTR, respectively) are characterized by a lower microbial diversity [8,9], viral infections and *Clostridium difficile* infections [10], and increased colonization by multi-drug resistant bacteria [11], but it is unknown whether the gut microbiome recovers in the long-term. Furthermore, transplant recipients often suffer from comorbidities and are exposed to polypharmacy, including proton-pump-inhibitors (PPIs), laxatives and antibiotics [8,12–14], which are all known to affect the gut microbiome and might exacerbate the dysbiosis [15]. In addition, the effect of the immunosuppressive drugs that recipients receive after transplantation, which impairs the host's immune system and therefore its capacity to control its gut microbiota, remain elusive [16].

Compelling evidence from allogeneic hematopoietic stem cell transplantation has shown that a reduced gut microbial diversity after transplantation is associated with the development of complications and

decreased recipient survival [17,18]. Disruption of the gut microbiota after hematopoietic stem cell transplantation was characterized by loss of diversity and domination by a single species, and a higher gut microbial diversity was associated with increased recipient survival. However, it is currently unknown whether the gut microbiome can be linked to recipient mortality in the setting of solid organ transplantation.

Previous studies on the gut microbiome in solid organ transplantation have been constrained by small sample sizes, lack of longitudinal and long-term data, and the use of 16S rRNA marker gene sequencing, which provides only limited information on microbial taxonomy and does not allow for functional characterization of the gut microbiome [10]. To overcome these limitations, we sequenced 1,370 fecal samples from 415 LTR and 672 RTR from the TransplantLines BioBank and Cohort study [19] using shotgun metagenomics. Of these, 78 RTR were followed starting prior to transplantation and at 3-, 6-, 12- and 24-months post transplantation. We also generated shotgun metagenomics data for 1,183 healthy, age-, sex- and BMI-matched control subjects from the Dutch Microbiome Project (DMP) as part of the Lifelines cohort [20] to quantify the extent of gut dysbiosis of ESLD and ESRD patients and LTR and RTR. We used these extensive data to address three major aims. The first aim was to test whether the severity of microbial dysbiosis following solid organ transplantation reduces the likelihood of recipient survival, as shown for allogeneic hematopoietic stem cell transplantation [17,18]. Our second aim was to expand on previous research describing the post-transplantation gut microbiota [8,10,11] via in-depth characterization of the gut microbiome using multiple layers and to examine the influence of intrinsic and external factors. Our third aim was to characterize the short-term dynamics of the host's gut microbiome during its transitions from end-stage disease to post-transplantation.

Results And Discussion

TransplantLines microbiome study

In this study, we collected fecal samples, performed metagenomic sequencing of the extracted DNA and profiled the gut microbiome of 2,553 participants, including 1,370 fecal samples from 415 LTR and 672 RTR from the TransplantLines BioBank and Cohort study [19]. The median time since transplantation was 9 years (interquartile range [IQR], 4-18) and 5.5 years (IQR, 1-12) for LTR and RTR, respectively. We also included 1,183 profiled metagenomes from identically processed samples from age-, sex- and BMI-matched healthy DMP controls (**Fig. 1**)[21]. To analyze the gut microbiome in end-stage disease, 87 ESLD and 78 ESRD patient samples were collected prior to transplantation. Longitudinal samples (N=361) were collected for the 78 ESRD patients at 3-, 6-, 12- and 24-months post-transplantation and used to characterize the short-term temporal dynamics following renal transplantation. Patient characteristics and immunosuppressive regimens are summarized in **Supplementary Table S1**, **Table S2** and **Table S3**. After quality control and filtering of the metagenomic sequencing data (**see Methods**), we retained a total of 384 taxa (8 phyla, 14 class, 20 order, 40 family, 83 genera and 219 species), 351 metabolic pathways,

215 virulence factors and 167 antibiotic resistance genes that exhibited a relative abundance of at least 1% and a prevalence of 10% across samples.

Gut dysbiosis is associated with increased mortality following solid organ transplantation

To characterize the gut microbiome of LTR and RTR following solid organ transplantation, we started by analyzing alpha and beta diversity in comparison to healthy controls. Previous studies have shown that the gut microbiome of both LTR and RTR exhibits dysbiotic characteristics [8,11]. We hypothesized that the extent of microbial alterations post transplantation may be associated with an increased recipient mortality, as previously shown for allogeneic hematopoietic stem cell transplantation [17]. To investigate this relationship, we first performed a principal component analysis of 328 LTR, 594 RTR and 1,183 healthy controls. In agreement with previous studies, we observed that the gut microbiota of LTR and RTR showed significantly lower diversity (Mann-Whitney U, $P_{RTR}=2.0x10^{-21}$; U=254,311 and $P_{LTR}=3.1x10^{-9}$; U=235,071; **Fig. 2B**) and altered microbial composition (PERMANOVA, $P_{LRT\ vs.\ healthy}=1x10^{-4}$, $P_{RTR\ vs.\ healthy}=1x10^{-4}$; **Fig. 2A**) compared to healthy controls. To further assess the association of gut dysbiosis with transplant recipient overall patient survival post transplantation, we performed a multivariate survival analysis controlling for recipient age, sex and the years since transplantation (**see Methods**). Similar to the previous analysis by Peled et al. [17] for allogeneic hematopoietic stem cell transplantation recipients, we first tested the association between microbial diversity and mortality. To do so, we stratified LTR and RTR into a high (Shannon diversity > 2.48; N=160) and low (Shannon diversity < 2.48; N=159) diversity groups based on the median Shannon diversity. In the low diversity group, we observed a significantly increased risk of post-transplant mortality for LTR (hazard ratio [HR], 2.91; 95% confidence interval [CI]: 1.03-8.16; P=0.04; adjusted HR: 2.96; 95% CI: 1.03-8.47; P=0.04). 96% of the recipients survived 3-years post-transplantation in the high diversity compared to 77% in the low diversity group (**Fig. 2C**). When we considered microbial diversity as a continuous variable, the association between microbial dysbiosis and mortality for LTR was even stronger: for every unit decrease in microbial diversity, the overall mortality risk increased by 45% (adjusted HR: 0.55; 95% CI: 0.37-0.79; $P=1.4x10^{-3}$; **Fig. 2D**). In contrast, we did not observe a significant association between gut microbial diversity and transplant recipient overall survival for RTR (adjusted HR: 1.19; 95% CI: 1.16-1.63; P>0.05; **Fig. 2F and 2G**).

To also allow for testing this association beyond microbial diversity, we quantified the Aitchison distance between the gut microbiota of transplant recipients and healthy controls. Compared to microbial diversity, the Aitchison distance is a measure of dissimilarity in microbial community composition. Here we found that a larger Aitchison distance to healthy controls was associated with an increased likelihood of death for both LTR (HR, 1.68; 95% CI, 1.27-2.23, $P=3.3x10^{-4}$, adjusted HR, 1.71; 95% CI, 1.27-2.31; $P=4.0x10^{-4}$; **Fig. 2E**) and RTR (HR, 1.41; 95% CI, 1.10-1.83, $P=9.2x10^{-3}$, adjusted HR, 1.69; 95% CI, 1.28-2.23; $P=1.7x10^{-4}$; **Fig. 2H**): with every unit increase in dissimilarity, the overall mortality risk increased by 71% for LTR and 69% for RTR. These results show that the likelihood of recipient overall survival decreases with the severity of microbial dysbiosis following liver and renal transplantation.

Post-transplantation gut microbiome is characterized by both taxonomic and metabolic alterations

To better understand the link between recipient post-transplant survival and microbiome alterations, we characterized the microbial species and pathways underpinning this association. To do so, we first modeled the relative abundance of microbial species using linear models, accounting for potential confounders including age, sex, BMI, smoking, and the use of PPIs, laxatives and antibiotics (**Supplementary Table 1, 2 and 3, and see Methods**). We found 102 species (55%) that were differentially abundant in LTR vs. healthy controls (FDR< 0.10), and 75 species (43%) that were differentially abundant in RTR vs. healthy controls. Of these, 60 differentially abundant species were shared between LTR and RTR, with all but two exhibiting the same direction of the relationship effect (*Bifidobacterium adolescentis* and *Eubacterium rectale* were increased in LTR vs. healthy controls but decreased in RTR vs. healthy controls). These results suggest that the gut dysbiosis observed following solid organ transplantation is at least partly underpinned by these 58 species. In agreement with this, Gupta et al. [22] and Gacesa et al. [21] reported several of these species as defining the 'unhealthy' gut microbiome. For example, compared to healthy controls, we found that both LTR and RTR suffered a reduction in the relative abundance of three species, *Sutterella wadsworthensis*, *Alistipes senegalensis* and *Bacteroidales sp.*, and an increase in the relative abundance of species such as *Ruminococcaceae sp.*, *Eggerthella lenta* and *Anaerotruncus colihominis*. Both LTR and RTR also had a significant expansion of *Escherichia coli,* which has previously been shown to increase the risk for *Escherichia* bacteriuria and urinary tract infection in RTR (**Fig. 3**; **Supplementary Table 4 and 5**) [23].

While these results suggest that the microbiota of transplant recipients changes relative to that of healthy controls, it does not tell us whether this is accompanied by a similar change in microbial metabolism. To test this, we modeled the relative abundance of microbial pathways using the same linear models as described above (**see Methods**). Here we found 284 pathways (82%) that were differentially abundant in LTR vs. healthy controls (FDR<0.10) and 224 pathways (64%) that were differentially abundant in RTR vs. healthy controls, with 200 pathways shared between LTR and RTR. While these included a variety of metabolic pathways related to amino acid metabolism, fatty acid metabolism, carbohydrate metabolism, nucleotide degradation and synthesis, and fermentation (**Supplementary Table 6 and 7**), we found evidence that the dysbiotic microbiota of LTR and RTR are accompanied by reduced butyrate production. More specifically, both LTR and RTR showed a reduction of two fermentation pathways (pyruvate fermentation to butanoate and acetyl CoA fermentation to butanoate II (PWY5676) and two flavin synthesis pathways (flavin biosynthesis I and III, both part of the vitamin B2 complex). The consequence of a reduced butyrate production is likely an impedance of the gut microbiome's anti-inflammatory response [24]. Lastly, we also found 11 quinone biosynthesis genes that were significantly increased in both LTR and RTR. While we can only speculate on the mechanisms underlying this observation, quinones are an important form of vitamin K_1 which is crucial in hemostasis and bone formation [25] (**Supplementary Tables 6 and 7**).

Gut microbiome of transplant recipients is enriched in antibiotic resistance genes and virulence factors

Due to the immunosuppressed state, both LTR and RTR frequently require antibiotic therapy, which could select for multi-drug resistant bacteria in the gut [26]. Annavajhala et al. [11] have even suggested that multi-drug resistant bacteria could act as a marker of gut dysbiosis. We therefore hypothesized that the gut microbiome of transplant recipients would be enriched with antibiotic resistance genes compared to the gut microbiome of healthy controls. We also investigated the levels of virulence factors in the gut microbiome of transplant recipients compared to healthy controls. Virulence factors are indicative of bacterial pathogenicity [27] and could therefore likely act as another important marker for gut dysbiosis.

We found that antibiotic resistance genes and virulence factors were more common and diverse in LTR and RTR compared to healthy controls (**Supplementary Tables 8-11**). Because both antibiotic resistance genes and virulence factors were extremely sparse in healthy controls, we could not apply the same linear models that we used for microbial species and pathways. Instead, we performed a logistic regression on presence-absences of antibiotic resistance genes or virulence factors with a prevalence cutoff at 1% across samples (**see Methods**). In LTR and RTR, 104 (71%) and 109 (67%) antibiotic resistance genes were more common compared to healthy controls, respectively (FDR<0.10). Of these, 93 antibiotic resistance genes were shared between LTR and RTR. For example, compared to healthy controls, both RTR and LTR were enriched with 36 different antibiotic resistance genes that code for efflux proteins, 17 for antibiotic inactivation genes, and 19 for antibiotic target alteration genes (**Supplementary Table 8 and 9**). Furthermore, both LTR and RTR had increased levels of TolC coding proteins which have the potential to drive antibiotic efflux for multiple classes of antibiotics ($FDR_{LTR}=9.3x10^{-9}$; $FDR_{RTR}=3.8x10^{-14}$). These results show that the resistome (all antibiotic resistance genes found in the gut microbiome) of the post-transplantation gut microbiome exhibits a higher richness than that of healthy controls.

Finally, 112 (53%) and 167 (52%) virulence factors were more common in LTR vs. healthy controls and RTR vs. healthy controls, respectively (FDR<0.10), and 85 virulence factors were shared between LTR and RTR. We found that multiple proteins, including adherence (VF0220, VF0222, VF0404) and adherence invasion (VF0221) proteins, and multiple iron uptake proteins (VF0123, VF0136, VF0227, VF0228, VF0229, VF0230 and VF0256), invasion proteins (VF0236, VF0237, VF0239) and type II/III secretion proteins (VF0116, VF0118, VF014, VF0333) were significantly increased in LTR and RTR compared to healthy controls (**Supplementary tables 10 and 11**). These results show that the dysbiotic gut microbiomes of LTR and RTR are enriched with proteins that can increase the pathogenic potential of the gut microbiota. Overall, the enrichment of both antibiotic resistance genes and virulence factors strongly indicates that the gut microbiome of transplant recipients is characterized by a dysbiotic, unhealthy state.

Phenotypes influencing the gut microbiome of transplant recipients

We next explored which intrinsic and external host factors may explain the observed microbial dysbiosis in LTR and RTR. We conducted Permutational Multivariate Analysis Of Variance (PERMANOVA) tests using 52 different phenotypic variables, including anthropological and clinical markers and medication. In these analyses, we included 328 LTR and 594 RTR samples, but due to the limited overlap of phenotypes between LTR and RTR, the analyses were performed separately for LTR and RTR. Of the 52

different phenotypes, 21 and 24 were statistically significant for LTR and RTR, respectively. These explained a total of 18.8% and 13.7% of the variation in the gut microbiota of LTR and RTR, respectively. The factor that explained most variation (4.2%) was recipient status (LTR, RTR, or healthy control; FDR=$4.0x10^{-04}$; **Fig. 4**; **Supplementary table 12**) followed by the use of mycophenolic acid (1%) and age (0.9%). Age, years since transplantation, occurrence of re-transplantation, and estimated glomerular filtration rate (eGFR), significantly explained variation in the gut microbiota of both LTR and RTR (FDR<0.10). Some phenotypic variables were unique to each transplant group. For example, diarrhea, liver enzymes as measured by alkaline phosphatase (ALP) and gamma-glutamyl transferase (GGT) and Troponin-T (indicative of ischemic heart injury) significantly explained variation in the microbiota of LTR. In contrast, phenotypic variables important for RTR included anti-hypertensive treatment, C-reactive protein (CRP), diabetes, BMI, fat percentage, body surface area (BSA), and handgrip strength, of which the latter relates to overall muscle status of an individual [28]. Biomarkers indicative of chronic heart failure, i.e. amino-terminal pro-B-type natriuretic peptide (NT-proBNP), also explained variation in the gut microbiota of RTR (FDR<0.10). Diabetes and CRP were significantly correlated with increased richness for both antibiotic resistance genes ($r_{diabetes}$=0.13, r_{CRP}=0.10, P<0.05) and virulence factors ($r_{Diabetes}$=0.14, r_{CRP}=0.07, P<0.05). Mychophenlic acid and the use of antibiotics significantly correlated with lower Shannon diversity ($r_{mychophenlic\ acid}$=-0.11, $r_{antibiotics}$=-0.07, P<0.05, respectively). Finally, all immunosuppressive drugs showed significant effects on the gut microbial community in both LTR and RTR (FDR<$1.0x10^{-4}$).

Immunosuppressive drugs as a driver of gut dysbiosis

Solid organ transplant recipients are in permanent need of immunosuppressive drugs post transplantation to prevent allograft rejection. In the previous section, we found that all different types of immunosuppressive drugs had a significant effect on the gut microbiota and could therefore be an important factor in the observed post-transplantation dysbiosis. To test their effect on the relative abundance of microbial species and metabolic pathways in users compared to non-users, we analyzed the different kinds of immunosuppressive drugs either individually, or in combination. In both analyses, we included the immunosuppressive drugs as fixed effect(s) while controlling for other confounders (**see Methods**). We focused on immunosuppressive drugs that were used individually or in combination by at least 100 transplant recipients (N=5: prednisolone, mycophenolic acid, azathioprine, cyclosporine, and tacrolimus; **Supplementary table 13**).

Testing the effect of each kind of immunosuppressive drug individually revealed 56 species (26%) and 157 metabolic pathways (45%) that were differentially abundant (**Fig. 5A**, FDR<0.10) between users and non-users across all kinds of immunosuppressive drugs. However, each kind of immunosuppressive drug also exhibited a unique pattern of differentially abundant species and pathways (**Supplementary table 14 and 15**). Prednisolone and mycophenolic acid users had the highest numbers of significantly differentially abundant species and pathways compared to azathioprine, cyclosporine and tacrolimus. This may reflect a power issue, since these two kinds of immunosuppressive drugs were the most

commonly used among the transplant recipients. We observed similar effects on the gut microbiomes of prednisolone and mycophenolic acid users, with three species (*Akkermansia muciniphila*; *Bifidobacterium adolescentis* and *Eubacterium rectale*) that are typically involved in the production of short chain fatty acids (SCFAs) were significantly decreased in their relative abundance (FDR<0.10; **Fig. 5C**) [29]. Correspondingly, prednisolone and mycophenolic acid users also exhibited a decrease in the pathways responsible for pyruvate fermentation (PWY108, PWY5100, PWY5676 and PWY6588, FDR<0.10). SCFAs play an important role in the immune system by inducing T regulatory cells in the human intestinal mucosa [29]. In tacrolimus-using recipients, we observed a higher relative abundance of *Roseburia intestinalis* which has been reported as a tacrolimus metabolizer [30].

In the second analysis, we tested the effect of 5 common combinations of immunosuppressive drugs (prednisolone and cyclosporin; prednisolone, mycophenolic acid, and tacrolimus; mycophenolic acid and tacrolimus; prednisolone and tacrolimus; prednisolone and mycophenolic acid; **Supplementary table 13**). We observed 47 species (21.5%) and 131 metabolic pathways (37.3%) that were differentially abundant (FDR<0.10; **Fig 5B**) between users and non-users across all 5 combination therapies (**Supplementary table 16 and 17**). A set of common commensal species—*A. muciniphila, R. intestinalis*, *E. rectale*, *E. eligens*, *B. adolescentis*, and *Butyrivibrio crossotus* was significantly altered (FDR<0.10). Consistent with the results from the previous analyses, these bacteria are involved in SCFA biosynthesis pathways [29]. In addition, all users exhibited a decrease in the relative abundance of the related SCFA pathways (CENTERM.PKWY and PWY 108; FDR<0.10; **Fig. 5D**). Lastly, *Bacteroides thetaiotaomicron*, a commensal bacteria that can become an opportunistic pathogen [31], was significantly increased in all 5 combination therapies. Overall, these results suggest that a complex interaction between immunosuppressive drugs and the gut microbiome contributes to the observed dysbiosis of post-transplantation recipients.

End-stage liver and renal disease are associated with two different dysbiotic community states

End-stage disease represents the pre-transplantation phase, with chronically ill patients waiting to undergo solid organ transplantation. Alterations in the gut microbiome of end-stage disease patients have already been described in both ESLD [6] and ESRD [7] patients. However, these studies had rather small sample sizes and used 16S rRNA marker gene sequencing, which does not allow for a functional characterization of the gut microbiome. We therefore compared the gut microbiome of pre-transplantation samples from 87 ESLD patients and 78 ESRD patients to the gut microbiomes of 1,183 healthy controls. In agreement with previous studies, a principal component analysis revealed that the gut microbiota associated with end-stage disease was markedly distinct from that of healthy controls (PERMANOVA: $P_{ESLD\ vs.\ healthy}=1.0x10^{-4}$; $P_{ESRD\ vs.\ healthy}=1.0x10^{-4}$), with the largest distance to healthy controls observed for the ESLD patients (**Fig. 6A**). Correspondingly, ESLD patients also exhibited lower microbial diversity than healthy controls (**Supplementary Figure 3,** Mann-Whitney, U=74,734, $P=1.2x10^{-12}$). A sub-analysis of underlying diseases and the severity of disease in relation to diversity did not reveal any strong associations (**Supplementary Figure 1**). Overall, these results suggest that the gut microbiome of both ESLD and ESRD patients have shifted to an unhealthy microbiota, represented by two different

dysbiotic community states (PERMANOVA: $P_{ESLD\ vs\ ESRD}=6.0x10^{-4}$**; Fig. 6A and 6B**). The observation of two distinct community configurations is not surprising given the underlying difference in both physiology and anatomy between ESLD and ESRD. On top of this, ESLD and ESRD patients are on different long-term medication regimes, including therapies for diabetes and hypertension [32,33].

To elucidate which microbial features were likely driving the observed dysbiotic states of ESLD and ESRD, we modeled the relative abundance of each feature using the same linear models approach described earlier. The gut microbiome of ESLD and ESRD patients exhibited markedly different patterns compared to healthy controls, with ESLD patients showing the largest shift away from healthy controls. The gut microbiome of ESLD and ESRD exhibited an altered abundance of 49 species (30%), 206 pathways (59%), 73 antibiotic resistance genes (45%) and 83 bacterial virulence factors (26%), whereas that of ESRD exhibited an altered abundance of 37 species (27%) and 126 pathways (37%), 4 antibiotic resistance genes (3%) and 2 virulence factors (1%) (FDR<0.10; **Supplementary Table 18-25**). While the total number of significantly differentially abundant features was higher in ESLD patients, there were 21 species that were shared with ESRD patients, including a significant decrease of the generally favorable species *Faecalibacterium prausnitzii*. Consistent with previous studies [6], ESLD-specific changes included an increase of several species from genera such as *Escherichia*, *Clostridium* and *Streptococcus*, while ESRD-specific alterations included an increase in the abundance of *Methanobrevibacter smithii*, a methane-producing archaea [34], and *Ruminococcus torques* which is known to decrease gut barrier integrity [35]. Lastly, ESLD and ESRD shared 44 differentially abundant metabolic pathways with similar directionality in their relationships (**Supplementary table 18-21**). Of these, 18 nucleosides and nucleotides biosynthesis pathways were significantly decreased and 10 amino acids biosynthesis pathways were significantly increased (FDR<0.10; **see Supplementary table 18-21**). While both ESLD and ESRD showed signs of taxonomic and metabolic dysbiosis, ESLD patients appeared to exhibit especially pronounced metabolic dysbiosis, with 59% of their microbial pathways altered compared to healthy controls (**see Supplementary Table 20 for full list)**.

Temporal development of the gut microbiome following transplantation

After solid organ transplantation, fewer complications may arise if the dysbiotic gut microbiome of end-stage disease is quickly ameliorated and restored. To move the field in this direction, we have to first understand the short-terms dynamics of the gut microbiome directly after transplantation and how it changes relative to the gut microbiome of end-stage disease patients (i.e., pre-transplantation) and healthy controls. To gain such an understanding, we analyzed 361 longitudinal samples from 78 end-stage disease patients who underwent renal transplantation. These RTR were then followed 3-, 6-, 12- and 24-months post transplantation (**Fig. 1**). Surprisingly, we observed that the gut microbiome 3 to 24 months after renal transplantation occupied the same dysbiotic state as the gut microbiome of end-stage disease (i.e., pre-transplantation; **Fig. 6A**), and this was the case for both microbial species and pathways. However, for species, we observed that the gut microbiome appeared to move closer to the pre-transplantation state as the time since the transplantation increased (**Fig. 6A and 6B**). Computation of

the Aitchison distance (in 2D Euclidean space) of rclr-transformed relative abundances at pre- and post-transplantation time points, as compared to the healthy controls, revealed that the distance to the healthy gut microbiota was indeed smallest for the pre-transplantation and 24-months post-transplantation samples (**Fig. 6A and 6B**). Interestingly, we observed the opposite pattern for pathways: the 3- and 24-months post-transplantation samples were the closest and farthest away from healthy controls, respectively. These patterns suggest that, while there is a sharp shift in the microbial community directly following solid organ transplantation, the functional potential of this community changes more gradually, likely in response to the immunosuppressive drugs the transplantation recipients are prescribed. Finally, consistent with extensive gut dysbiosis following solid organ transplantation, we observed a significantly lower Shannon diversity at all post-transplantation time points compared to the pre-transplantation samples (P<0.01; **Supplementary figure 3**). To confirm whether these short-term changes persist long-term, we analyzed all the microbiome data of recipients who underwent solid organ transplantation. This analysis revealed even as long as 20 years after transplantation the gut microbiome of transplant recipients shows a reduced microbial diversity and altered composition (**Supplementary figure 2A and 2B**).

We next analyzed which microbial species were responsible for the short-term dynamical patterns described above. In these analyses, we also included RTR for whom the post-transplantation gut microbiome was characterized 3-, 6-, 12-, or 24-months following transplantation (**see Methods for more information**). These analyses revealed 24 species (11%) that were differentially abundant in the gut microbiota post-transplantation compared to pre-transplantation (FDR<0.10; **Supplementary table 26**). Plotting log-ratios comparing the rclr-transformed relative abundance of each microbial species at a post-transplantation time point to that at pre-transplantation revealed how these features changed following transplantation compared to pre-transplantation (**Fig. 6C**). For example, the relative abundance of many species that are generally considered to be commensal, such as *A. muciniphila, B. adolescentis* and *Ruminococcus obeum* consistently decreased post-transplantation compared to pre-transplantation (**Fig. 6C**). Other species such as *C. asparagiforme, Bilophila wadsworthia* and *Coprobacter fastidiosus* exhibited increased relative abundances post-transplantation compared to pre-transplantation (**Fig. 6C**; **Supplementary table 26**). Overall, these results suggest that the gut microbiota directly following organ transplantation is experiencing additional perturbations that result in an increased state of dysbiosis.

We also found signs of metabolic dysbiosis in the gut microbiome directly following solid organ transplantation. The abundances of 125 metabolic pathways (35.5%) was significantly altered in the gut microbiome post-transplantation compared to pre-transplantation (FDR<0.10; **see Supplementary table 27**). These pathways could be further classified into 29 metabolic classes, responsible for degradation, biosynthesis and energy metabolism (**Fig. 6C**). The direction of the relationships post-transplantation compared to pre-transplantation were generally stable, either increasing or decreasing, with few exceptions (**Fig. 6C**; **Fig. S5**). Similar to the cross-sectional results, we found evidence for a decreased butyrate production, with the relative abundance of the pathways responsible for pyruvate fermentation to butanoate (FDR<0.10 for 6M, 12M, 24M) and acetyl CoA fermentation to butanoate II (FDR<0.10 for 6M) significantly decrease compared to pre-transplantation. Also similar to the cross-sectional results, we

found 25 differentially abundant quinone biosynthesis pathways. Lastly, the number of differentially abundant antibiotic resistance genes (N=16 or 3.7%; **Supplementary table 28**) and bacterial virulence factors (N=11 or 2.8%; **Supplementary table 29**) were much smaller in this longitudinal analysis compared to the cross-sectional analysis (3.7% vs 28.3% and 2.8% vs 27.7%, respectively), and this difference is likely the consequence of an increasing cumulative exposure to doses of antibiotics in the years following organ transplantation [36].

Conclusion

This is the largest study to date on the gut microbiome both prior to and following solid organ transplantation and including both cross-sectional and longitudinal data. We show that the gut microbiome of transplant recipients does not revert back to a state comparable to that of healthy controls. Instead, the post-transplantation gut microbiome is characterized by a reduced microbial diversity, a gain of pathogens at the expense of commensal bacteria, a decrease in the abundance of important metabolic pathways, and an increase in the diversity and prevalence of antibiotic resistance genes and virulence factors. These findings have potentially far-reaching implications—we show that immunosuppressive drugs are the single most important factor underpinning the observed gut dysbiosis, and that the severity of dysbiosis is associated with a reduced likelihood of recipient survival. While a larger prospective study of LTR and RTR is required to confirm our findings, we are the first to report for the first time a significant association between the gut microbiome and overall recipient mortality in the setting of solid organ transplantation. Similarly, as is suggested by recent data in the setting of hematopoietic stem cell transplant recipients, fecal microbiota transplantation directly following solid organ transplantation may help to restore the gut microbiome and thereby improve health outcomes and overall recipient survival [17,37,38].

Using our longitudinal data, we lay important groundwork in characterizing the short-term dynamics of the gut microbiome following solid organ transplantation as it transitions from end-stage disease to post-transplantation. We find that while there is a sharp shift in the microbiota directly following solid organ transplantation, the functional potential of this community changes more gradually, likely in response to the immunosuppressive drugs. Finally, while promising breakthroughs are being made in the field of pharmacomicrobiomics [14,39], more research on the complex interaction between the gut microbiome and immunosuppressive drugs is needed in order to improve health outcomes for solid organ transplant recipients. Overall, our study represents an important step forward towards microbiome-targeted interventions that could potentially change the outcome of solid organ transplantation.

Methods

Study Cohorts

Ethical approval

All participants signed an informed consent form prior to sample collection. TransplantLines (METc 2014/077) and LifeLines (METc 2017/152) were approved by the institutional ethics review board (IRB) from the University Medical Center Groningen (UMCG). Both studies adhere to the UMCG Biobank Regulation and are in accordance with the World Medical Association (WMA) Declaration of Helsinki and the Declaration of Istanbul.

TransplantLines microbiome study

We recruited adult patients with end-stage liver or renal disease (i.e. pre-transplantation) and patients that had undergone a liver or renal transplantation. These patients provided fecal samples to the TransplantLines microbiome study (Trial registration number NCT03272841). TransplantLines is a unique and novel prospective biobank and cohort study within the UMCG which is the largest transplantation center in the Netherlands. A detailed description of the TransplantLines study is given in the design paper by Eisenga et al. [19]. Briefly, we prospectively recruited adult patients (age ≥ 18 years) undergoing liver or renal transplantation between June 2015 and August 2019. We included patients who underwent a transplantation before June 2015 in the observational part of our study. A subset of subjects from the Dutch Microbiome Project (DMP)[21] was included as a control group. These subjects are part of the LifeLines cohort which consists of 167,000 subjects from the Northern part of the Netherlands. Control subjects were matched with transplantation patients based on age, sex and BMI. Fecal samples from TransplantLines and DMP were processed with the same DNA extraction protocols and sequencing platform (see below).

Clinical and Laboratory Characteristics

A fixed set of laboratory parameters was measured at every study visit and were included in the study database with the patients consent. Blood samples were taken prior to the study visit in the morning after 8 - 12 hours overnight fasting. Demographic characteristics along with data on medication use were provided by the participants and verified with the patients during the study visit. General medical information at the time of transplantation was extracted from electronic hospital records. Blood pressure was measured according to a standard clinical protocol and automatic device (Philips Suresign VS2+, Andover, Massachusetts, USA). Anthropometry measurements included length, body weight and fat percentage (multifrequency bioelectrical impedance device; BIA, Quadscan 4000, Bodystat, Douglas, British Isles). Hand grip strength was assessed with a Jamar Hydraulic Hand Dynamometer (Patterson Medical JAMAR 5030J1, Warrenville, Canada) [28]. Multiple questionnaires were used: ROME III was used to assess the presence of functional diarrhea or irritable bowel syndrome [40], alcohol use was assessed with the Alcohol Use Disorders Identification Test (AUDIT) in liver patients and smoking was assessed using the Smoking Behaviour Questionnaire. Clinical markers were measured using in hospital routine assays from the fasting blood sample.

Immunosuppressive Drugs

Continuous exposure to treatment with immunosuppressive drugs is necessary for prevention of rejection of the transplanted organ. According to a standardized protocol, there are five main immunosuppressive drugs that were used in the analysis including prednisone/prednisolone, mycophenolic acid, tacrolimus, cyclosporine and azathioprine. Sirolimus and everolimus were used less frequently and were not included in the analysis. To acquire adequate immunosuppression a combination of immunosuppressive drugs is used in clinical practice [41]. Therefore, we also analyzed the effect of combinations of immunosuppressive drugs on the gut microbiome. Postoperative immunosuppression regimen in the liver and renal transplant sub-cohort has been listed in Supplementary Table 1.

Longitudinal and cross-sectional sampling

The combined cross-sectional and longitudinal design of TransplantLines allowed us to analyze the gut microbiome of end-stage disease patients, short term effect of on the post-transplantation microbiome and the long-term effect on the post-transplantation microbiome. Transplantation candidates are screened extensively prior to transplantation. A patient was included in the prospective part of the study if the patient was eligible for transplantation. Pre-transplantation patients were allowed as end-stage disease patients. Further study visits were performed at 3 months, 6 months, 12 months and 24 months post-transplantation. Transplant recipients that were before June 2015 were included in the cross - sectional part of the study for one study visit. The patients in the cross-sectional part of the study were not followed prospectively and were included at a time point > 1-year post-transplantation.

Microbiome data generation

Fecal sample collection and subsequent processing

Patients were asked to collect a fecal sample the day prior to the TransplantLines visit. A FecesCatcher (TAG Hemi VOF, Zeijen, The Netherlands) was sent to the patients at home. Feces were collected and stored in appropriate tubes and frozen immediately after collection. The participant transported the frozen fecal sample in cold storage (with ice cubes or in a cooler) to the TransplantLines visit the following day. Subsequently, the fecal sample was immediately stored at −80°C. Participants in the Dutch microbiome project produced, collected, and froze fecal samples at home using standardized stool collection kits provided by UMCG. Frozen fecal samples were collected by UMCG personnel and frozen within 15 minutes after production, transported on dry ice and stored at UMCG at -80^{o}C until DNA extraction.

DNA extraction

Microbial DNA was extracted using QIAamp Fast DNA Stool Mini Kit (Qiagen, Germany) according to the manufacturer's instructions. The QIAcube (Qiagen, Germany) automated sample preparation system was used for this purpose.

PCR amplification, library construction and Illumina sequencing

Library preparation was performed using NEBNext® Ultra™ DNA Library Prep Kit for Illumina for samples with total DNA amount lower than 200ng, as measured using Qubit 4 Fluorometer, while samples with DNA yield higher than 200ng were prepared using NEBNext® Ultra™ II DNA Library Prep Kit for Illumina®. Libraries were prepared according to the manufacturer's instructions. Metagenomic shotgun sequencing was performed using Illumina HiSeq 2000 sequencing platform and generated approximately 8 Gb of 150 bp paired-end reads per sample (mean 7.9 gb, st.dev 1.2 gb). Library preparation and sequencing were performed at Novogene, China.

Metagenomic data processing

Illumina adapters and low-quality reads (Phred score <30) were filtered out using KneaData (v0.5.1). Then Bowtie2 (v2.3.4.1) was used to remove reads aligned to the human genome (hg19). The quality of the reads was examined using FastQC toolkit (v0.11.7). Taxonomy alignment was done by MetaPhlAn2 (v2.7.2) against the database of marker genes mpa_v20_m200. Metacyc pathways were profiled by HUMAnN2 (v0.11.1). Bacterial virulence factors and antibiotic resistance genes were identified using shortBRED (shortbred_identify.py (v0.9.5) and shortbred_quantify.py tool (v0.9.5)) against virulence factors of pathogenic bacteria (VFDB) database (http://www.mgc.ac.cn/VFs/main.htm) and comprehensive antibiotic resistance database (CARD) (https://card.mcmaster.ca/) separately. Samples were further excluded by criteria that eukaryotic or viral abundance > 25% of total microbiome content or total read depth < 10 million. In total, we identified 1132 taxa (17 phyla, 27 class, 52 order, 98 family, 231 genera and 705 species), 586 metabolic pathways, 313 virulence factors and 957 antibiotic resistance genes. With 10% percent present rate and 0.01% relative abundance threshold, 384 taxa (8 phyla, 14 class, 20 order, 40 family, 83 genera and 219 species), 351 metabolic pathways, 323 virulence factors and 167 antibiotic resistance genes were left after filtering. Total-sum normalization was applied to all microbiome data after filtering. Analyses were performed using locally installed tools and databases on CentOS (release 6.9) on the high-performance computing infrastructure available at UMCG and University of Groningen (RUG). An example of scripts used for microbiome process is available at https://github.com/GRONINGEN-MICROBIOME-CENTRE/Groningen-Microbiome/tree/master/Projects/DMP/microbiome_profiling

Statistical analyses

Compositional data analysis

High-throughput DNA sequencing produces compositional data, which means that information can only be obtained in the form of relative abundances that are independent of the total microbial load in a given sample [42]. This means that an observed increase of one microbial feature necessarily requires a decrease for another feature. If this data property is not accounted for, the analyst risk of introducing false-positives and spurious correlations [42–45] While standard statistical methodology assumes that the analyzed data are represented by variables free to vary from - to within Euclidean space [46], compositional data occupies the simplex which is a restricted space where variables are strictly positive

and vary from 0 to 1 if data are represented as proportions, or 0 to 100 if data are represented as percentages [46]. A log-ratio transform places such data in a log-ratio coordinate space known as the Aitchison geometry in which standard statistical methodology can be applied [42,47,48]. After such a transformation, the only information that can be obtained from the data about changes in the abundance of features are in the form of log-ratios [49] with the denominator serving as the reference frame; this means that a change in the relative abundance of a given feature (i.e. the numerator) is always relative to a reference frame (i.e. the denominator) given by one or multiple other features [43].

Robust Aitchison PCA via DECOIDE

We applied the robust centered log-ratio (rclr) transformation on our abundance matrix using the DECOIDE program [43]. The rclr is simply the centered log-ratio (clr) transformation defined only on non-zero counts. Therefore, the benefit of using the rclr rather than the clr-transformation is that it circumvents the need for zero-imputation. More formally, the rclr-transformation for a sample can be obtained by

$$x_{rclr} = [log(\frac{x_1}{g_r(x)}), log(\frac{x_2}{g_r(x)}), \ldots, log(\frac{x_D}{g_r(x)})] \qquad \text{(eq. 1)}$$

where $x = [x_1, x_2, x_3, \ldots, x_D]$ denotes a sample containing D "counted" features (e.g. species or pathways), and $g_r(x)$ is the geometric mean defined only on observed features in the focal sample, and serves as the reference frame.

Furthermore, the Euclidean distance between rclr-transformed samples is called the Robust Aitchison distance [46]. Importantly, this distance satisfies all properties required for compositional data analysis [46], such as scale invariance and sub-compositional coherence [50,51]. These two properties are especially important for microbiome analysis: scale invariance guarantees that the analyst can treat two communities as equivalent if they have the same relative abundances, even if they have different total abundances. Sub-compositional coherence guarantees that the conclusions of the analysis is not affected by the subset of features analyzed; for example, the results from only including common features would not be changed by the addition of rare ones. Consequently, the Aitchison distance outperforms other commonly used distance metrics such as Bray-Curtis and Jensen-Shannon divergence [52,53].

The DECOIDE [43] program takes an abundance table and performs the rclr-transformation, generates the Aitchison distance matrix and applies a dimensionality reduction through Robust PCA on only the non-zero values of the data [53]. We ran the stand-alone version of the DECOIDE program in Python (3.8.6) using the auto-rcpa option which estimates the optimal number of principal components from the data. In our case, the algorithm found a rank of 2 to be the most parsimonious low-rank representation.

Survival analyses

We assessed the association between gut microbial diversity and all-cause mortality using multivariable Cox proportional hazard models adjusting for patient age, sex and years since transplantation. We analyzed both the association between all-cause mortality and (1) gut microbial diversity and (2) the gut community dissimilarity (i.e. the Aitchison distance) between transplant recipients and healthy controls. For diversity, patients were stratified into high-diversity and low-diversity groups according to the median Shannon diversity, and the relationship of each group with patient mortality was determined using Kaplan-Meier curves for LTR and RTR separately. The continuous variables (i.e. Shannon diversity and the distance to healthy controls) were scaled to unit variance prior to the analysis. Analyses of all-cause mortality were presented as hazard ratios with 95% CIs. Finally, we checked whether each included variable independently satisfied the assumptions of the Cox model by computing the Schoenfeld residuals (P>0.05). For the survival analysis we used the survival and the rms R package.

PERMANOVA via adonis

To test whether different community configurations observed in the PCA plots were statistically different from each other (e.g. ESLD vs healthy controls samples), we conducted Permutational Multivariate Analysis Of Variance (PERMANOVA) tests on the Aitchison distances generated by DECOIDE. PERMANOVA tests were also used to test the explanatory power of a total of 52 different phenotypic variables on the post-transplant gut microbiome (i.e. LTR and RTR). We used the adonis function from the R package vegan with 9999 permutations.

Differential abundance analysis with Linear Models

To perform differential abundance analysis, we modeled the rclr-transformed relative abundances of microbial species and pathways using linear models accounting for potential confounders such as age, sex, BMI, smoking, and the use of proton pump inhibitor (PPI), laxatives and antibiotics (**Supplementary Table 1, 2 and 3**). This included the differential abundance analysis comparing features in (1a) LTR vs healthy controls; (1b) RTR vs healthy controls; (2a) ESLD vs healthy controls; (2b) ESRD vs healthy controls; (3) immunosuppressive drugs: users vs non-users; and (4) post-transplantation vs to pre-transplantation for renal transplantation patients. In (3), we tested five immunosuppressive drugs individually between users and non-users (prednisolone; tacrolimus; mycophenolic acid; azathioprine; and cyclosporin), and five drugs in combination between users and non-users (cyclosporin and prednisolone; mycophenolic acid, tacrolimus and prednisolone; mycophenolic acid and tacrolimus; tacrolimus and prednisolone; mycophenolic acid and prednisolone; **Supplementary table 13**). In the differential abundance analysis (1), (2) and (3), we used linear models (using the lm function in R) only including fixed effects. While in (4), we used linear mixed models (using the lmer function from lmerTest R package) including subject id as a random effect. Lastly, because both antibiotic resistance genes and virulence factors were extremely sparse in healthy controls, we could not apply the same linear models that we used for microbial species and pathways. Instead, we performed logistic regression models on presence-absences of antibiotic resistance genes or virulence factors with a prevalence cutoff at 1%. Apart from this, the differential analysis (1) and (2) was performed the same. Statistical significance was

determined after each differential analysis by correcting for multiple testing (n=features) using a false discovery rate (FDR) of 0.10 with the p.adjust(..., method="BH") function in R.

Log-ratio analysis of species post vs pre-transplantation

Using our longitudinal data, we constructed log-ratios comparing each microbial species' rclr-transformed relative abundance at a time point post-transplantation to its rclr-transformed relative abundance at pre-transplantation. These log-ratios were constructed by subtracting each focal species' average rclr-transformed relative abundances across all post transplantation samples from it's averaged rclr-transformed relative abundances across all pre transplantation samples. More formally, let

$\widehat{x_{i,t}^{rclr}}$

denote the average rclr-transformed relative abundance for microbial species at post-transplantation time point , which is given by

$$\widehat{x_{i,t}^{rclr}} = \frac{1}{n}\sum_{j=1}^{n} x_{t,j}^{rclr} = \frac{x_{t,1}^{rclr} + x_{t,2}^{rclr} + \cdots + x_{t,n}^{rclr}}{n} \qquad (\text{eq. } 2)$$

Then, the log-ratio of species 's average rclr-transformed relative abundance at post-transplant time point to its average rclr-transformed relative abundance at pre-transplantation (preTx), is given as follows

$$log\left(\frac{x_{i,t}}{x_{i,preTx}}\right) = \frac{1}{n}\sum_{j=1}^{n} x_{t,j}^{clr} - \frac{1}{n}\sum_{j=1}^{n} x_{preTx,j}^{clr} \qquad (\text{eq. } 3)$$

Data and code availability

Raw sequencing data and corresponding metadata that support the findings of this study are available on request from the corresponding author R.K.W. The participant metadata is not publicly available as they contain information that could compromise research participant privacy/consent. The authors declare that all other data supporting the findings of this study are available within the paper and its supplementary information files. The code to analyze reproduce the findings are available at https://github.com/GRONINGEN-MICROBIOME-CENTRE/Groningen-Microbiome/tree/master/Projects

Declarations

Acknowledgements

The authors wish to acknowledge the services of the Lifelines Cohort Study, the contributing research centers delivering data to Lifelines, and all the study participants. The Lifelines Biobank initiative has been made possible by subsidy from the Dutch Ministry of Health, Welfare and Sport, the Dutch Ministry

of Economic Affairs, the University Medical Center Groningen (UMCG the Netherlands), University of Groningen and the Northern Provinces of the Netherlands. We would like to thank the Center for Information Technology of the University of Groningen (RUG) for their support and for providing access to the Peregrine high performance computing cluster, and the Genomic Coordination Center (UMCG and RUG) for their support and for providing access to Calculon and Boxy high performance computing clusters. Metagenomics library preparation and sequencing was done at Novogene. We also thank K. Mc Intyre for English and content editing.

Author contribution

JCS, YL, SH drafted the first version of the manuscript. JCS, JRB and RKW wrote and finalized subsequent versions of the manuscript. All authors critically revised and approved the final version of the manuscript. JCS, SH, JRB and RG performed the statistical analyses. RG designed and implemented metagenomic data analysis pipelines. AVV, AP assisted in other statistical analyses, interpretation of data and drafting of the manuscript. RMD, MFE, AWGN, DK, VC, MAYK, AK, AP, TJK, BHJ, SPB, JSFS, MRHF, RJP, FJCC, VEdM, CW, EAMF, AZ, JF, HJMH, HB, SJLB and RKW collected data, assisted in study planning and critically reviewed the manuscript. HJMH, HB, SJLB and RKW, conceived, coordinated and supported the study.

Funding

Sequencing of the LifeLines cohort and the liver part of the TransplantLines cohort was funded by a grant from the CardioVasculair Onderzoek Nederland grant (CVON 2012-03) to MH, JF and AZ. Sequencing of the kidney part of the TransplantLines cohort was funded by a grant from the Dutch NWO/TTW/DSM partnership program Animal Nutrition and Health (project number 14939) to SJLB. RG was supported by the collaborative TIMID project (LSHM18057-SGF) financed by the PPP allowance made available by Top Sector Life Sciences & Health to Samenwerkende Gezondheidsfondsen (SGF) to stimulate public-private partnerships and co-financing by health foundations that are part of the SGF. RKW is supported by the Seerave Foundation and the Dutch Digestive Foundation (16-14). AZ is supported by the ERC Starting Grant 715772, Netherlands Organization for Scientific Research NWO-VIDI grant 016.178.056, the Netherlands Heart Foundation CVON grant 2018-27, and the NWO Gravitation grant ExposomeNL 024.004.017. VEdM is supported by Netherlands Organization for Scientific Research NWO-VENI grant 09150161810030, JF is supported by NWO Gravitation Netherlands Organ-on-Chip Initiative (024.003.001), the ERC Consolidator grant 101001678 and the Netherlands Heart Foundation CVON grant 2018-27. CW is further supported by a European Research Council (ERC) advanced grant (ERC-671274) and an NWO Spinoza award (NWO SPI 92-266). LC is supported by a joint fellowship from the University Medical Center Groningen and China Scholarship Council (CSC201708320268) and the Foundation De Cock-Hadders grant (20:20-13).

Competing interests declaration

Authors declare no conflict of interest.

Scripts and availability of data:

Scripts used for data analysis can be found at:

https://github.com/GRONINGEN-MICROBIOME-CENTRE/GroningenMicrobiome/tree/master/Projects

References

1. Tullius, S. G. & Rabb, H. Improving the Supply and Quality of Deceased-Donor Organs for Transplantation. *The New England journal of medicine* vol. 379 693–694 (2018).
2. Chong, A. S. & Alegre, M.-L. The impact of infection and tissue damage in solid-organ transplantation. *Nat. Rev. Immunol.* **12**, 459–471 (2012).
3. Mori, D. N., Kreisel, D., Fullerton, J. N., Gilroy, D. W. & Goldstein, D. R. Inflammatory triggers of acute rejection of organ allografts. *Immunol. Rev.* **258**, 132–144 (2014).
4. Wu, H.-J. & Wu, E. The role of gut microbiota in immune homeostasis and autoimmunity. *Gut Microbes* **3**, 4–14 (2012).
5. Sommer, F., Anderson, J. M., Bharti, R., Raes, J. & Rosenstiel, P. The resilience of the intestinal microbiota influences health and disease. *Nat. Rev. Microbiol.* **15**, 630–638 (2017).
6. Acharya, C. & Bajaj, J. S. Chronic Liver Diseases and the Microbiome: Translating Our Knowledge of Gut Microbiota to Management of Chronic Liver Disease. *Gastroenterology* (2020) doi:10.1053/j.gastro.2020.10.056.
7. Wang, X. *et al.* Aberrant gut microbiota alters host metabolome and impacts renal failure in humans and rodents. *Gut* **69**, 2131–2142 (2020).
8. Swarte, J. C. *et al.* Characteristics and Dysbiosis of the Gut Microbiome in Renal Transplant Recipients. *J. Clin. Med. Res.* **9**, (2020).
9. Lee, J. R. *et al.* Gut microbiota dysbiosis and diarrhea in kidney transplant recipients. *Am. J. Transplant* **19**, 488–500 (2019).
10. Baghai Arassi, M., Zeller, G., Karcher, N., Zimmermann, M. & Toenshoff, B. The gut microbiome in solid organ transplantation. *Pediatr. Transplant.* **24**, e13866 (2020).
11. Annavajhala, M. K. *et al.* Colonizing multidrug-resistant bacteria and the longitudinal evolution of the intestinal microbiome after liver transplantation. *Nature Communications* vol. 10 (2019).
12. Zimmermann, M., Zimmermann-Kogadeeva, M., Wegmann, R. & Goodman, A. L. Mapping human microbiome drug metabolism by gut bacteria and their genes. *Nature* **570**, 462–467 (2019).
13. Vila, A. V. *et al.* Impact of commonly used drugs on the composition and metabolic function of the gut microbiota. *Nat. Commun.* **11**, 1–11 (2020).
14. Weersma, R. K., Zhernakova, A. & Fu, J. Interaction between drugs and the gut microbiome. *Gut* **69**, 1510–1519 (2020).

15. Shaw, L. P. *et al.* Modelling microbiome recovery after antibiotics using a stability landscape framework. *ISME J.* **13**, 1845–1856 (2019).
16. Gibson, C. M., Childs-Kean, L. M., Naziruddin, Z. & Howell, C. K. The alteration of the gut microbiome by immunosuppressive agents used in solid organ transplantation. *Transpl. Infect. Dis.* e13397 (2020).
17. Peled, J. U. *et al.* Microbiota as Predictor of Mortality in Allogeneic Hematopoietic-Cell Transplantation. *N. Engl. J. Med.* **382**, 822–834 (2020).
18. Shono, Y. & van den Brink, M. R. M. Gut microbiota injury in allogeneic haematopoietic stem cell transplantation. *Nat. Rev. Cancer* **18**, 283–295 (2018).
19. Eisenga, M. F. *et al.* Rationale and design of TransplantLines: a prospective cohort study and biobank of solid organ transplant recipients. *BMJ Open* **8**, e024502 (2018).
20. Scholtens, S. *et al.* Cohort Profile: LifeLines, a three-generation cohort study and biobank. *Int. J. Epidemiol.* **44**, 1172–1180 (2015).
21. Gacesa, R. *et al.* The Dutch Microbiome Project defines factors that shape the healthy gut microbiome. *Cold Spring Harbor Laboratory* 2020.11.27.401125 (2020) doi:10.1101/2020.11.27.401125.
22. Gupta, V. K. *et al.* A predictive index for health status using species-level gut microbiome profiling. *Nat. Commun.* **11**, 4635 (2020).
23. Magruder, M. *et al.* Gut uropathogen abundance is a risk factor for development of bacteriuria and urinary tract infection. *Nat. Commun.* **10**, 5521 (2019).
24. Liu, H. *et al.* Butyrate: A Double-Edged Sword for Health? *Adv. Nutr.* **9**, 21–29 (2018).
25. Ellis, J. *et al.* Investigation of Vitamin K Quinone Metabolism by Human Gut Bacteria. *Curr Dev Nutr* **4**, 392–392 (2020).
26. Sabino, Y. N. V. *et al.* Characterization of antibiotic resistance genes in the species of the rumen microbiota. *Nat. Commun.* **10**, 5252 (2019).
27. Yang, J., Chen, L., Sun, L., Yu, J. & Jin, Q. VFDB 2008 release: an enhanced web-based resource for comparative pathogenomics. *Nucleic Acids Res.* **36**, D539–42 (2008).
28. Angst, F. *et al.* Prediction of grip and key pinch strength in 978 healthy subjects. *BMC Musculoskelet. Disord.* **11**, 94 (2010).
29. Ohira, H., Tsutsui, W. & Fujioka, Y. Are Short Chain Fatty Acids in Gut Microbiota Defensive Players for Inflammation and Atherosclerosis? *J. Atheroscler. Thromb.* **24**, 660–672 (2017).
30. Guo, Y. *et al.* Commensal Gut Bacteria Convert the Immunosuppressant Tacrolimus to Less Potent Metabolites. *Drug Metab. Dispos.* **47**, 194–202 (2019).
31. Ulger Toprak, N., Celik, C., Cakici, O. & Soyletir, G. Antimicrobial susceptibilities of Bacteroides fragilis and Bacteroides thetaiotaomicron strains isolated from clinical specimens and human intestinal microbiota. *Anaerobe* **10**, 255–259 (2004).

32. Weir, M. R. & Fink, J. C. Safety of medical therapy in patients with chronic kidney disease and end-stage renal disease. *Curr. Opin. Nephrol. Hypertens.* **23**, 306–313 (2014).
33. Liou, I. W. Management of end-stage liver disease. *Med. Clin. North Am.* **98**, 119–152 (2014).
34. Samuel, B. S. *et al.* Genomic and metabolic adaptations of Methanobrevibacter smithii to the human gut. *Proc. Natl. Acad. Sci. U. S. A.* **104**, 10643–10648 (2007).
35. Cani, P. D. Metabolism in 2013: The gut microbiota manages host metabolism. *Nat. Rev. Endocrinol.* **10**, 74–76 (2014).
36. Li, J. *et al.* Antibiotic Treatment Drives the Diversification of the Human Gut Resistome. *Genomics Proteomics Bioinformatics* **17**, 39–51 (2019).
37. DeFilipp, Z. *et al.* Third-party fecal microbiota transplantation following allo-HCT reconstitutes microbiome diversity. *Blood Adv* **2**, 745–753 (2018).
38. Kakihana, K. *et al.* Fecal microbiota transplantation for patients with steroid-resistant acute graft-versus-host disease of the gut. *Blood* **128**, 2083–2088 (2016).
39. Doestzada, M. *et al.* Pharmacomicrobiomics: a novel route towards personalized medicine? *Protein Cell* **9**, 432–445 (2018).

Methods references

40. Ford, A. C. *et al.* Validation of the Rome III criteria for the diagnosis of irritable bowel syndrome in secondary care. *Gastroenterology* **145**, 1262–70.e1 (2013).
41. Hartono, C., Muthukumar, T. & Suthanthiran, M. Immunosuppressive drug therapy. *Cold Spring Harb. Perspect. Med.* **3**, a015487 (2013).
42. Gloor, G. B., Macklaim, J. M., Pawlowsky-Glahn, V. & Egozcue, J. J. Microbiome Datasets Are Compositional: And This Is Not Optional. *Front. Microbiol.* **8**, 2224 (2017).
43. Morton, J. T. *et al.* Establishing microbial composition measurement standards with reference frames. *Nat. Commun.* **10**, 2719 (2019).
44. van den Boogaart, K. G. & Tolosana-Delgado, R. Fundamental Concepts of Compositional Data Analysis. in *Analyzing Compositional Data with R* (eds. van den Boogaart, K. G. & Tolosana-Delgado, R.) 13–50 (Springer Berlin Heidelberg, 2013).
45. Lovell, D., Müller, W., Taylor, J., Zwart, A. & Helliwell, C. Proportions, percentages, ppm: do the molecular biosciences treat compositional data right. *Compositional data analysis. Wiley, Chichester* (2011).
46. Pawlowsky-Glahn, V. & Egozcue, J. J. Compositional data and their analysis: an introduction. *Geological Society, London, Special Publications* **264**, 1–10 (2006).
47. Pawlowsky-Glahn, V. & Egozcue, J. J. Geometric approach to statistical analysis on the simplex. *Stoch. Environ. Res. Risk Assess.* **15**, 384–398 (2001).
48. Aitchison, J. *The Statistical Analysis of Compositional Data*. (Springer Netherlands, 1986).

49. Egozcue, J. J. & Pawlowsky-Glahn, V. Groups of Parts and Their Balances in Compositional Data Analysis. *Math. Geol.* **37**, 795–828 (2005).
50. Aitchison, J. On criteria for measures of compositional difference. *Math. Geol.* **24**, 365– 379 (1992).
51. Chong, F. & Spencer, M. Analysis of relative abundances with zeros on environmental gradients: a multinomial regression model. *PeerJ* **6**, e5643 (2018).
52. Aitchison, J., Barceló-Vidal, C., Martín-Fernández, J. A. & Pawlowsky-Glahn, V. Logratio Analysis and Compositional Distance. *Math. Geol.* **32**, 271–275 (2000).
53. Martino, C. *et al.* A Novel Sparse Compositional Technique Reveals Microbial Perturbations. *mSystems* **4**, (2019).

Figures

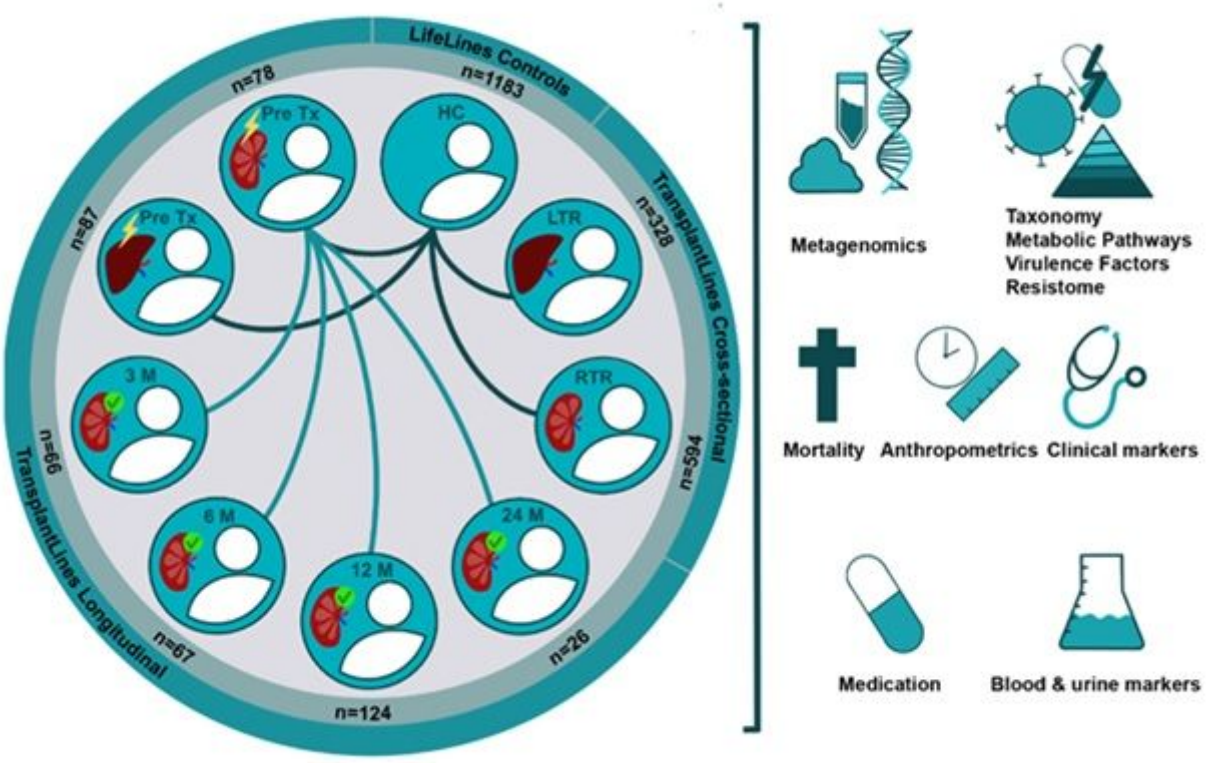

Figure 1

Schematic diagram of the TransplantLines microbiome study. The left panel shows an overview of the samples, including the healthy DMP controls (matched on age, sex and BMI). The right panel shows an overview of the phenotypes included in the study. Abbreviations: n=number of fecal samples; PreTx= pre-transplantation; HC=healthy controls; LTR=liver transplant recipient; RTR=renal transplant recipient; M= post-transplantation time point.

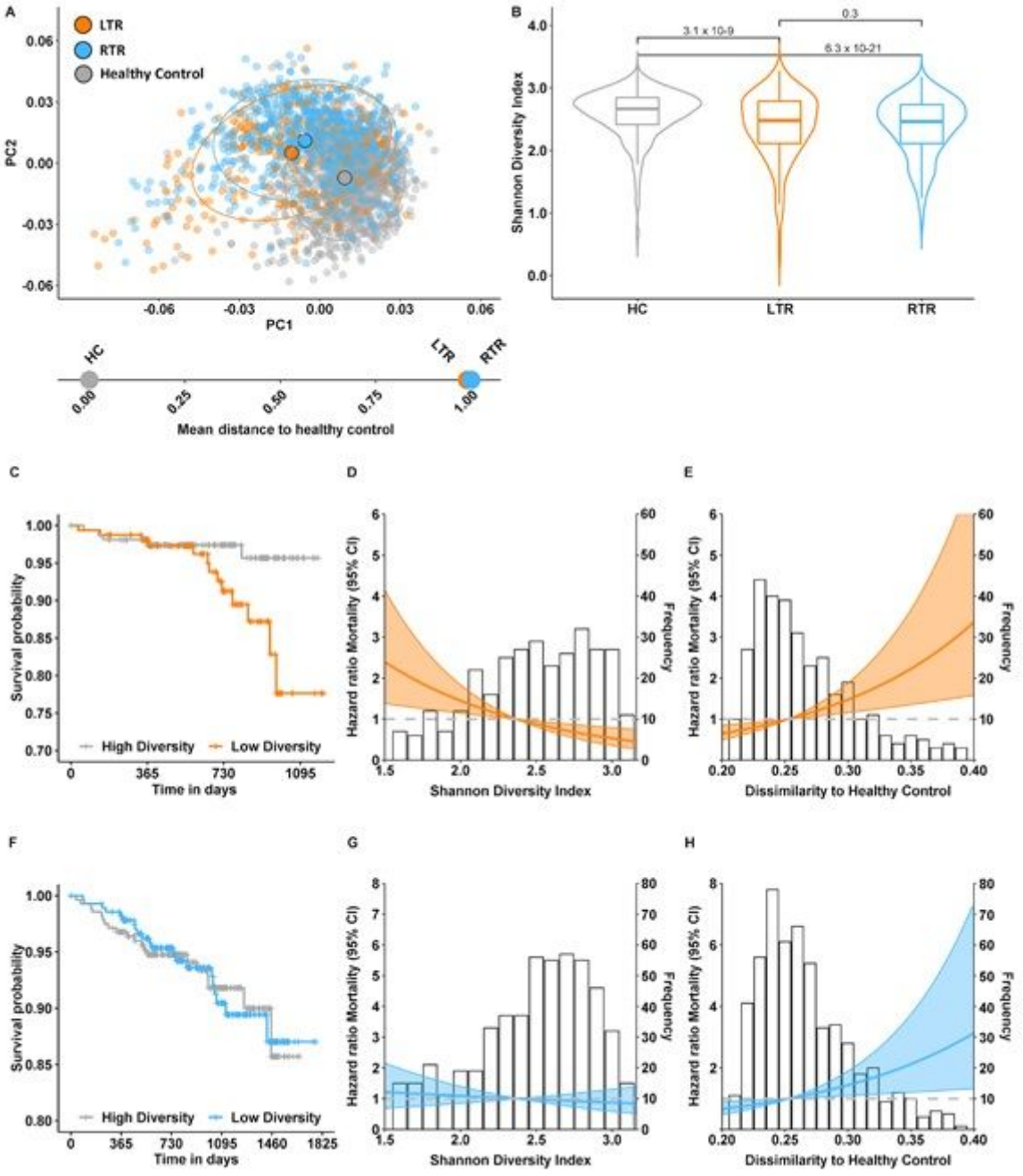

Figure 2

Overall post-transplant mortality increases with the severity of microbial dysbiosis following solid organ transplantation. (A) Principal components reflect Aitchison distances from species-level rclr-transformed relative abundances generated with DECOIDE 53. Blue, orange and gray dots represent renal transplant recipients (RTR), liver transplant recipients (LTR) and healthy controls (HC), respectively. Large dots represent the centroid of each group. The bottom panel depicts the Aitchison distance to healthy subjects, normalized between 0-1 with 1 representing the maximum distance. (B) Violin plots depict the Shannon diversity index in healthy controls (HC; gray), RTR (blue) and LTR (orange). Numbers reflect FDR corrected p-values: both LTR and RTR were statistically different compared to HC (PRTR vs HC = 6.3x10-21; PLTR vs

HC = 3.1x10-9). (C and F) Kaplan-Meier survival curves of overall mortality stratified by the median Shannon diversity index for (C) LTR (orange) and (F) RTR (blue). There were 18 deaths in total among 314 LTR and 42 deaths in total among 625 RTR. (D and G) Graphical representation of the association between Shannon diversity and all-cause mortality in (D) LTR (orange) and (G) RTR (blue). The lines show the adjusted hazard ratio (HR) and the shaded area corresponds to the 95% pointwise confidence interval (CI). The analyses were adjusted for age, sex, andyears since transplantation (P=1.4x10-3 and P>0.05 in LTR and RTR, respectively). (E and H) Graphical representation of the association of the Aitchison distance to healthy controls and all-cause mortality in (D) LTR (orange) and (G) RTR (blue). The lines show the adjusted hazard ratio (HR) and the shaded area corresponds to the 95% pointwise confidence interval (CI). The analyses were adjusted for age, sex, years since transplantation (P=4.0x10-4 and P=1.7x10-4 in LTR and RTR, respectively).

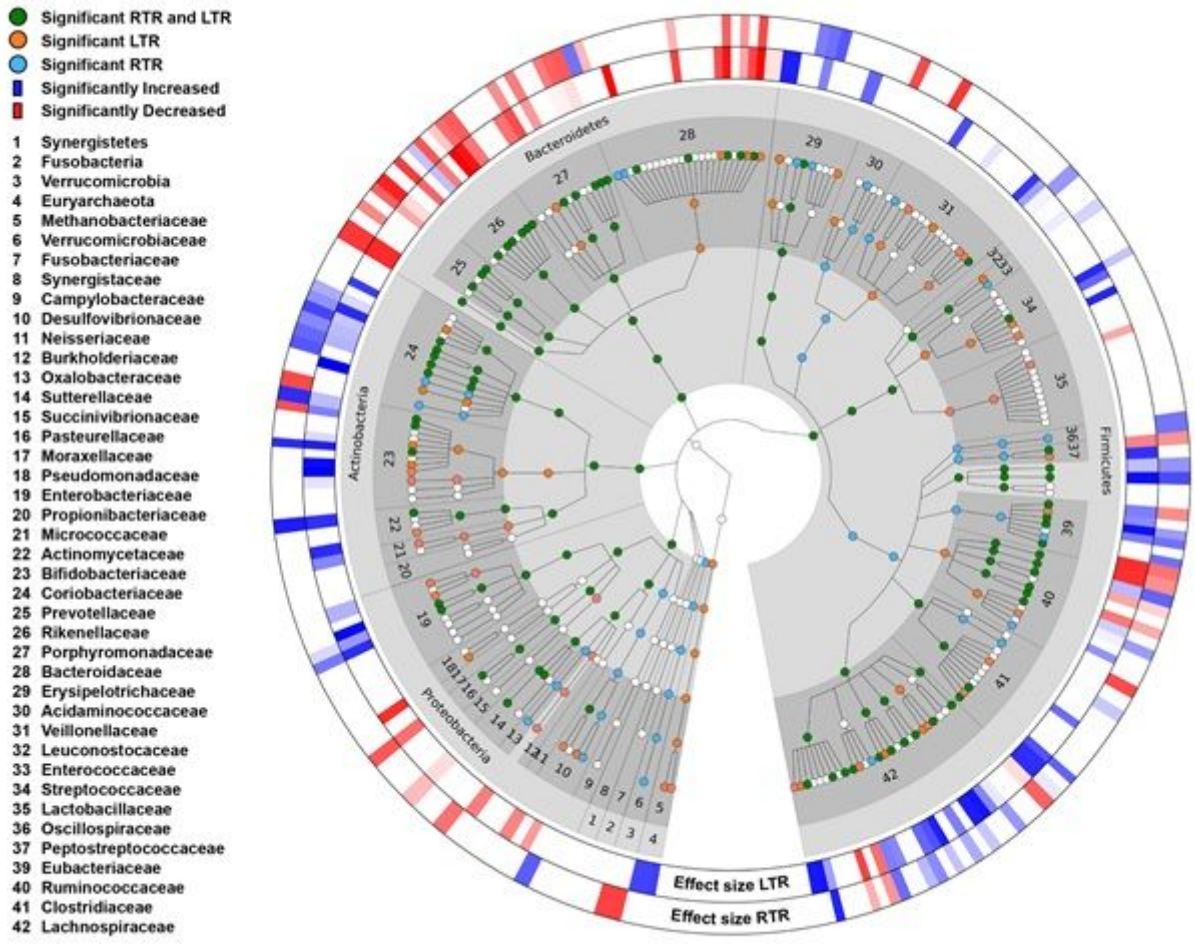

Figure 3

Characterization of significantly altered taxa compared to healthy controls in the post-transplantation gut microbiome. The cladogram depicts the results from multiple differential abundance analyses for LTR vs HC and RTR vs HC. From the inner to the outer circles, each taxonomic level is depicted ranging from domain (inner circle) to species-level (outer circle). Each dot represents a significantly differentially abundant taxon. The dots are colored to indicate significance; green, blue, and orange colors represent

significantly differentially abundant taxa shared between LTR and RTR, only significant in RTR and only significant in LTR, respectively. Bars in blue and red represent species whose relative abundance significantly increased and decreased, respectively.

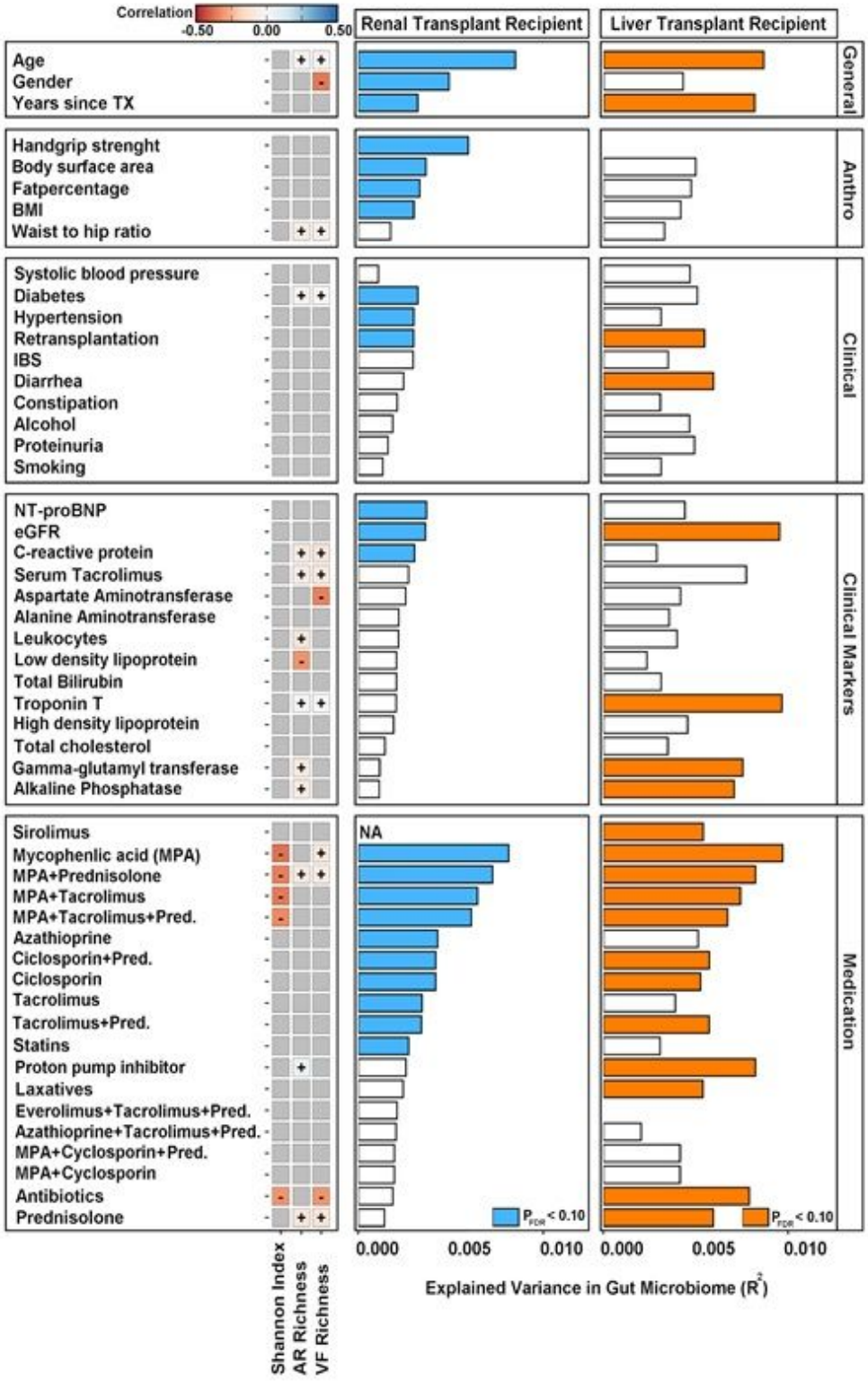

Figure 4

Intrinsic and external factors associated with inter-individual variation of the post-transplantation gut microbiome. Depicted are the general, anthropological, clinical, clinical markers and medication

phenotypes for both LTR and RTR. Correlation to the Shannon diversity index and pathway-, antibiotic resistance genes- and virulence factor richness is depicted in the heat map. Significant spearman correlations are colored by the strength of the correlation and + and - are representing the direction of the observed correlation. Grey squares indicate non-significant correlations (PFDR < 0.10) The bar plots show the explained variance for each phenotype for LTR (orange) and RTR (blue). Significance is indicated by filled bars (PFDR < 0.10). TX: transplantation, IBS: irritable bowel syndrome, eGFR: estimated glomerular filtration rate, MPA: mycophenolic acid and Pred.: prednisolone, AR: antibiotic resistance genes, VF: virulence factors.

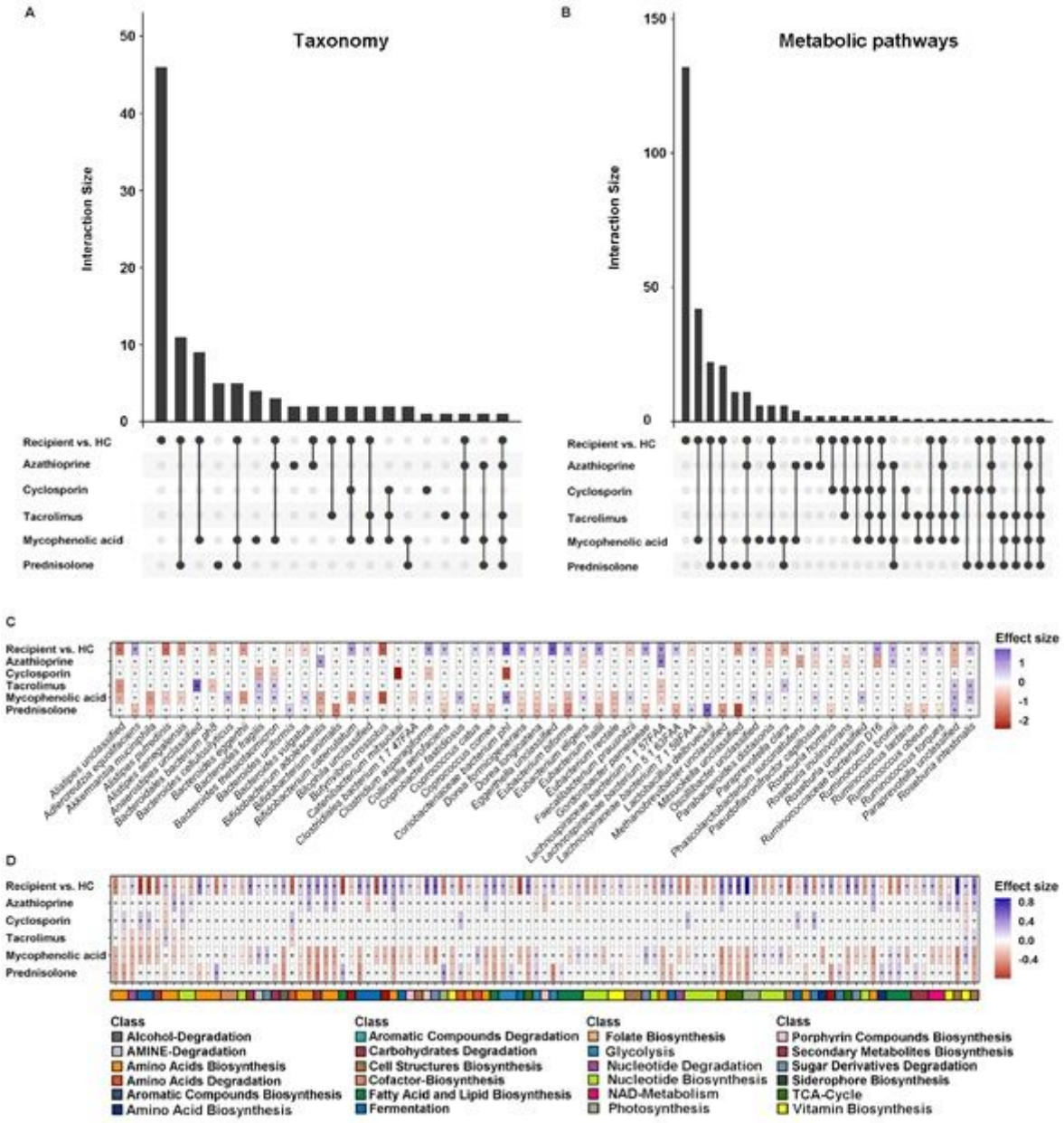

Figure 5

The effect of Immunosuppressive drugs on gut microbial composition and predicted pathways. (A and B) depicts the number of shared (A) species and (B) metabolic pathways between LTR and RTR that were significant in logistic regression models between user and non-user for each immunosuppressive drug or

combination therapy. C, D, Using taxon (C) and metabolic pathway (D) specific linear models we observed multiple features that were significantly enriched between user and non-user (PFDR<0.10). The heatmap depicts the effect size for each immunosuppressive drug or combination therapy with the direction of the relationship indicated by a + or -. Pathways are annotated from class to category. To disentangle the transplantation effect, we added the results for differential abundance analysis for transplant recipients (RTR and LTR) per feature in the last column of the heatmap.

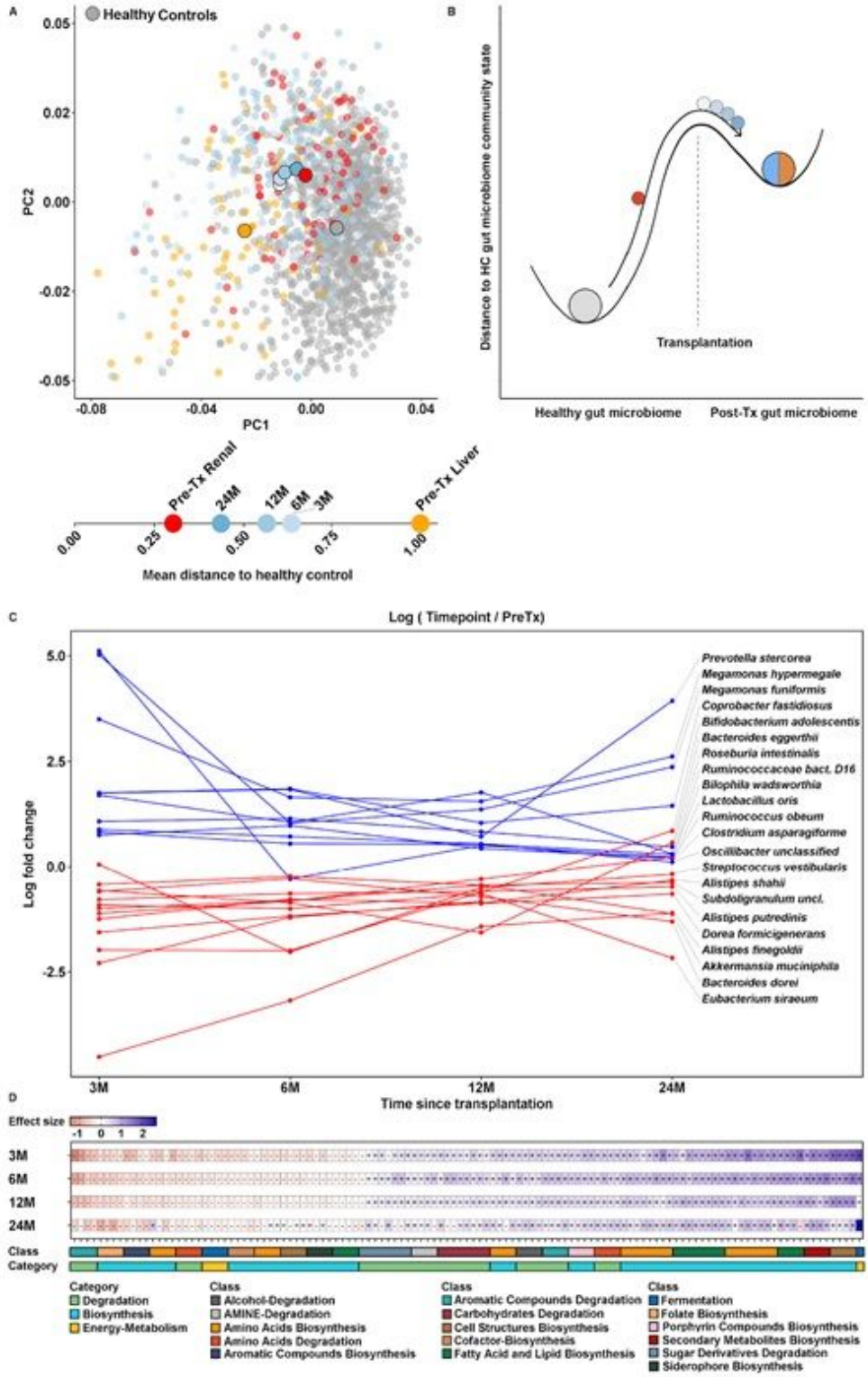

Figure 6

(A) Principal components reflect Aitchison distances from species-level rclr-transformed relative abundances generated with DECOIDE 43. Orange, red and grey dots represent pre-transplant liver (Pre-Tx Liver), pre-transplant renal (Pre-Tx Renal) and healthy controls (HC), respectively. The Large dots represent the centroid of each group. The dots in the blue color gradient depict renal samples collected 3-, 6-, 12-, and 24-months following transplantation. The bottom panel depicts the Aitchison distance to healthy subjects, normalized between 0-1 with 1 representing the maximum distance. The gut microbiome of ESRD (Pre-Tx Renal) patients is most similar to the gut microbiome of HC, however still significantly different. The microbiome of ESLD patients is most dissimilar compared to HC. For ESRD patients the gut microbiome partially restores but remains significantly different from HC post-transplantation (3-, 6-, 12-, 24- months post-transplantation vs HC, (B) A cup in the ball diagram depicting a shift in the gut microbiome from healthy controls to post-transplantation. The length of the x-axis represents possible states of the gut microbiome with a healthy state shown as the grey ball, and the unhealthy dysbiotic microbiome shown as the bicolored blue-orange ball. The y-axis represents the gut microbiome state in terms of taxonomic and functional composition and diversity. The distance from the origin represents the distance from this healthy state to that of the alternative dysbiotic community states. Using both cross-sectional and longitudinal data, we were able to study the transition of the gut microbiome pre- to post-transplantation, here shown as the smaller sized balls; the red ball indicate pre-transplantation, and the blue-gradient balls represent the transition in the 24 first months post-transplantation. (C) Log-ratios comparing each microbial species's rclr-transformed relative abundance at a time point post-transplantation to pre-transplantation. Lines in blue and red depicts a positive and negative log fold change, respectively, which means that compared to pre-transplantation the focal species increased/decreased post-transplantation. (D) Using pathway-specific linear mixed models we observed 122 pathways whose relative abundance were significantly altered compared to pre-transplantation (PFDR < 0.1). The heatmap depicts the effect size of the post-transplantation time point (3-, 6-, 12- and 24 months post-transplantation) compared to the pre-transplantation, with the direction of the relationship indicated by + or -. The color-coded lines depict which functional classes and categories the pathways belong to.

Supplementary Files

This is a list of supplementary files associated with this preprint. Click to download.

- SupplementaryTables.xlsx
- SupplementaryFigures.pdf